Lithuanian Journal of Physics
Vol. **65**, No. 1, pp. 24–31 (2025)
ISSN 1648-8504 eISSN 2424-3647
DOI: https://doi.org/10.3952/physics.2025.65.1.1

ELECTRON-IMPACT IONIZATION FOR Kr ATOM

A. Kynienė, V. Paberžis, Š. Masys, and V. Jonauskas

Institute of Theoretical Physics and Astronomy, Vilnius University, Saulėtekio 3, 10257 Vilnius, Lithuania
Email: ausra.kyniene@tfai.vu.lt

Received 9 November 2024; revised 1 December 2024; accepted 2 December 2024

Electron-impact ionization cross sections for the ground level of the Kr atom are studied using the scaled distorted-wave (DW) approximation. It is demonstrated that the DW cross sections calculated in the potential of the ionizing ion overestimate the experimental data at low and medium energies of the impacting electron. The scaled DW results, that include in calculations the value of the ionization threshold provided by National Institute of Standards and Technology, lead to good agreement with the measurements. A negligible contribution from the indirect process of the ionization to the total ionization cross sections is obtained in the final results. The study demonstrates that the higher ionization stages appear as a result of the ejection of additional electrons from the atomic system by the sequential ionization.

Keywords: atomic data, ionization, krypton

1. Introduction

Krypton is found in stellar atmospheres [1], interstellar medium [2, 3], planetary nebulae [4] and white dwarfs [5], and it is important for understanding cosmic abundances and star formation. Additionally, Kr plays a critical role in practical applications, such as lighting technologies [6, 7], gas lasers [8], and medical imaging systems [9].

Accurate modelling of plasma processes relies on a comprehensive understanding of charge state distribution within the plasma. Intensities of spectral lines emitted in high temperature environments depend on charge state population. Electron-impact ionization and recombination are crucial mechanisms that define the charge state distribution in the collisional plasmas.

Electron-impact ionization for the Kr atom was previously analyzed by several experimental groups. Rapp and Englander-Golden [10] measured the cross sections for the Kr atom from the ionization threshold up to 1000 eV using the total charge production method. The condense technique was used by Schram et al. to measure ionization cross sections from 0.6 to 20 keV [11] and from 100 to 600 eV [12]. Nagy et al. [13] presented the absolute ionization cross sections for the energies of impacting electron ranging from 0.5 to 5 keV. The fast beam technique was applied by Wetzel et al. [14] to analyze cross sections from the ionization threshold up to 200 eV. The pulsed beam and ion extraction techniques to measure ionization cross sections from the ionization threshold up to 1000 eV were employed by Krishnakumar and Srivastava [15]. The electron-impact ionization cross sections were measured using crossed electron beams and the time-of-flight mass spectrometer from 18 to 466 eV by Syage [16]. The total electron-impact ionization cross sections were defined from measured electron-impact ionization and photoionization ratios by Sorokin et al. [17]. The electron-impact ionization cross sections were analyzed from 140 to 4000 eV. Kobayashi et al. [18] obtained the ionization cross sections using a pulsed electron beam and pulsed ion extraction from the threshold up to 1 keV. Rejoub et al. [19] presented their results from the ionization threshold up to 1000 eV and discussed errors compared to previous measurements.

It should be noted that Rapp and Englander-Golden [10] and Scram et al. [11, 12] presented measurements for total ionization cross sections for the Kr atom. This means that these measurements include single and higher ionization stages.

Theoretically, the ionization of the Kr atom was previously analyzed using various approaches (for example, Ref. [20–23]). The distorted-wave (DW) calculations performed by Loch et al. [23] showed overestimated results compared to measurements.

The aim of the current work is to study electron-impact ionization cross sections from the ground level of the Kr atom. Analysis is performed using the scaled DW approximation. Direct and indirect ionization processes are analyzed and compared to available experimental data.

The rest of the paper is organized as follows. Section 2 presents a brief outline of the theoretical approach. In Section 3, the obtained results are discussed. Finally, we end with the conclusions from the present investigation.

2. Theoretical approach

The single ionization process is investigated as a result of direct and indirect processes,

$$\sigma_{if} = \sigma_{if}^{\mathrm{CI}} + \sum_k \sigma_{ik}^{\mathrm{CE}} B_{kf}^{\mathrm{a}}, \tag{1}$$

where $\sigma_{if}^{\mathrm{CI}}$ and $\sigma_{if}^{\mathrm{CE}}$ correspond to collisional ionization (CI) and collisional excitation (CE) cross sections, respectively. The excitation is a result of transition from the level i to the autoionizing level k. The produced level k can decay through radiative and Auger transitions. The single ionization is produced by autoionization from the level k to the level f of the subsequent ion. Therefore, the excitation with autoionization (EA) corresponds to the indirect process studied in this work.

The autoionization branching ratio is determined as a part of population transferred from the level k of the Kr atom to the level f of the Kr^+ ion,

$$B_{kf}^{\mathrm{a}} = \frac{A_{kf}^{\mathrm{a}}}{\Sigma_m A_{km}^{\mathrm{a}} + \Sigma_n A_{kn}^{\mathrm{r}}}, \tag{2}$$

where A_{km}^{α} and A_{kn}^{r} are Auger and radiative transition probabilities, respectively. The total lifetime of the level k is associated with the inverse of value in the denominator of Eq. (2). Excitations to the states k below the ionization threshold do not lead to the single ionization process. Therefore, the branching ratio is equal to zero for the levels k below the ionization threshold.

The direct ionization of the Kr atom is analyzed by taking into account the 4*s* and 4*p* subshells

$$[\mathrm{Ar}]3d^{10}4s^2 4p^6 + e^- \rightarrow$$
$$\rightarrow [\mathrm{Ar}]\begin{cases} 3d^{10}4s^2 4p^5 \\ 3d^{10}4s^1 4p^6 \end{cases} + 2e^-. \tag{3}$$

Here [Ar] means an Ar-like electron structure, i.e. 1*s*, 2*s*, 2*p*, 3*s*, 3*p* orbitals are fully occupied. The removal of electrons from the deeper than 4*s* and 4*p* subshells leads to the autoionizing states of the Kr^+ ion, which decay further to the higher ionization stages. Therefore, these subshells are not considered in this work.

Excitations from the 4*s* and 4*p* subshells are studied to calculate contribution from the indirect process:

$$[\mathrm{Ar}]3d^{10}4s^2 4p^6 + e^- \rightarrow$$
$$\rightarrow [\mathrm{Ar}]\begin{cases} 3d^{10}4s^2 4p^5 nl \\ 3d^{10}4s^1 4p^6 nl \end{cases} + 2e^-. \tag{4}$$

Here $n \le 20$, $l < n$, $l \le 4$. The excitations from the 3*d* subshell lead to the autoionizing states with energies exceeding the double ionization threshold for the Kr atom and, therefore, are not included in the study of the EA process.

The DW cross sections are multiplied by an energy dependent factor in this work to explain the experimental data. The scaling factor for the CI process includes the energy ε of the impacting electron, the ionization energy I and the kinetic energy of the bound electron ε_k:

$$\sigma_{ij}^{\mathrm{CI*}}(\varepsilon) = \frac{\varepsilon}{\varepsilon + I + \varepsilon_k} \sigma_{ik}^{\mathrm{CI}}(\varepsilon). \tag{5}$$

Here the star superscript represents the scaled DW cross sections. It should be noted that a slightly different expression for the scaling factor is used analyzing the CI cross sections of near neutral ions [24, 25].

The scaling factor used for excitation incorporates the electron energy ε, the transition energy ΔE_{ik} and the binding energy ε_{b} of the electron:

$$\sigma_{ij}^{\mathrm{CI*}}(\varepsilon) = \frac{\varepsilon}{\varepsilon + \Delta E_{ij} + \varepsilon_{\mathrm{b}}} \sigma_{ij}^{\mathrm{CE}}(\varepsilon). \tag{6}$$

Previously, the scaled DW cross sections were applied to explain the experimental data for the C atom and C^+ ion [24], Fe^{3+} [26], Si [27] and N [25] atoms. It should be noted that various scaling corrections to the cross sections were also used in other calculations to analyze measurements [28–32].

Energy levels, radiative and Auger transition probabilities as well as electron-impact excitation and ionization cross sections are studied using the Flexible Atomic Code (FAC) [33]. The code implements the Dirac–Fock–Slater (DFS) approximation. The *jj*-coupling scheme is used to generate configuration state functions. The excitation and ionization cross sections are analyzed using the DW approximation.

3. Results

Ionization cross sections for the ground level of the Kr atom obtained in the potential of the ionized ion are compared to the experimental data in Fig. 1. The presented theoretical values overestimate the experimental data at electron energies from the ionization threshold approximately up to the peak of the cross sections. However, the experimental results are underestimated by theory at higher energies of the impacting electron.

Theoretical ionization cross sections obtained in the potential of the ionizing ion are above measurements by a factor of 2.5 at peak values (Fig. 2). On the other hand, theoretical and experimental data converge to each other going to higher energies of the impacting electron. The scaling factors are applied to the DW cross sections and the results are presented in Fig. 3. The theoretical data are still above the measurements; however, the position of the peak is in good agreement with the peak from the measurements. The difference among the theoretical and experimental data can be explained by the difference in the single ionization thresholds. The theoretical ionization threshold of 12.77 eV is below by 1.23 eV from the value provided by National Institute of Standards and Technology (NIST) [34]. A similar tendency for the DFS ionization thresholds compared to the NIST data was also obtained for other atoms and ions: Si [27], N [25], Se^{2+} [35], Se^{3+} [36, 37], W^{25+} [38], W^{26+} [39, 40] and W^{27+} [41]. It was previously demonstrated that the incorporation of the NIST value for the ionization threshold in calculations leads to a better agreement of the theoretical cross sections with the experimental ones [27, 25].

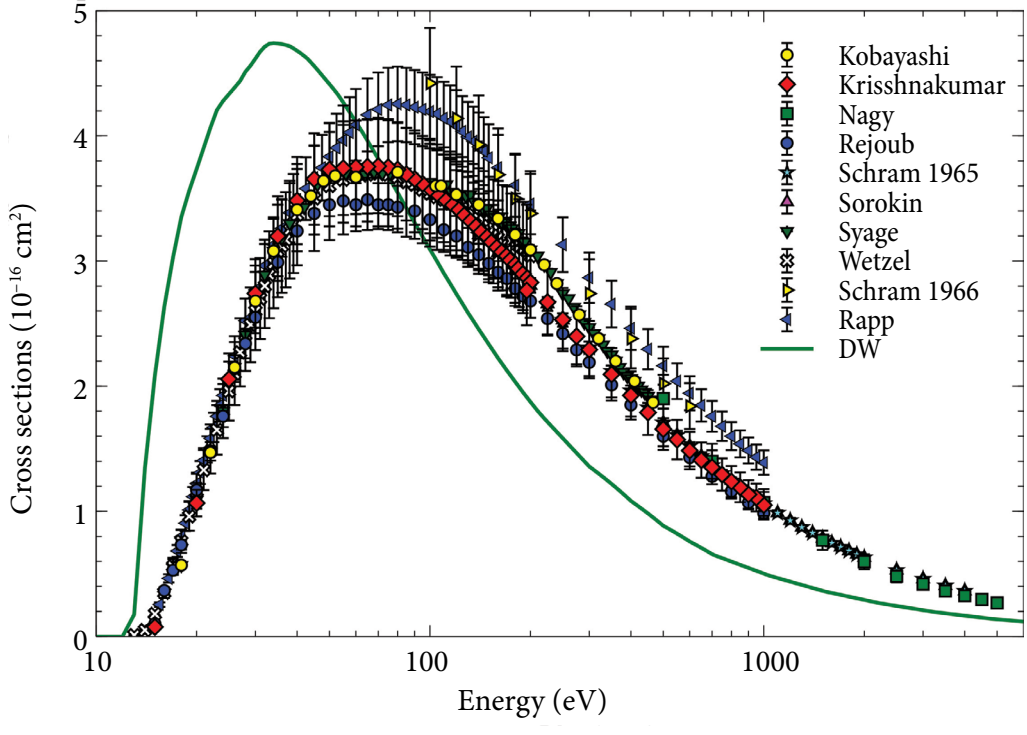

Fig. 1. DW cross sections compared to the experimental data. DW cross sections obtained in the potential of the ionized ion.

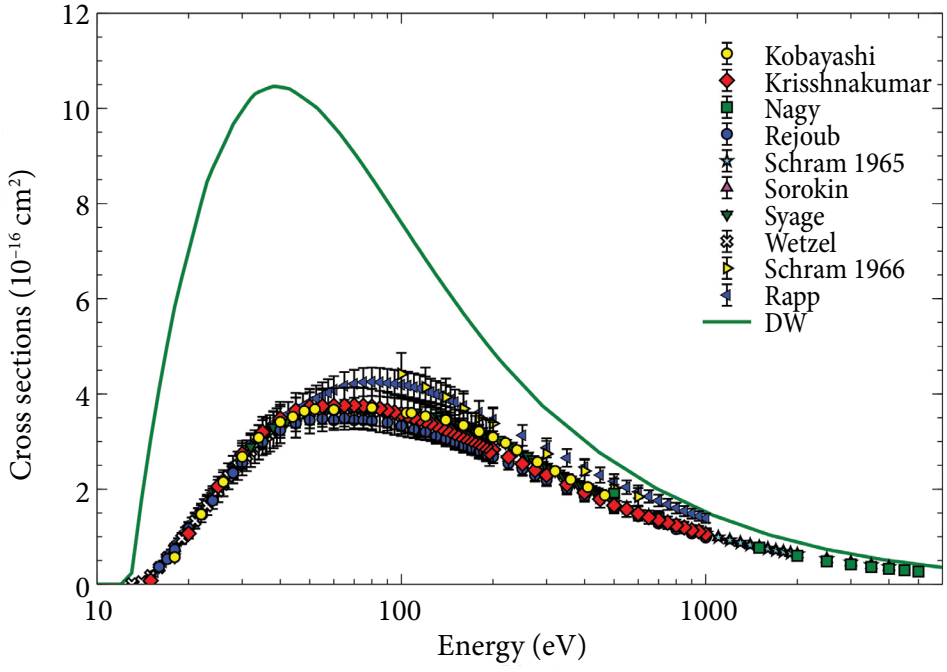

Fig. 2. DW cross sections compared to the experimental data. DW cross sections obtained in the potential of the ionizing ion.

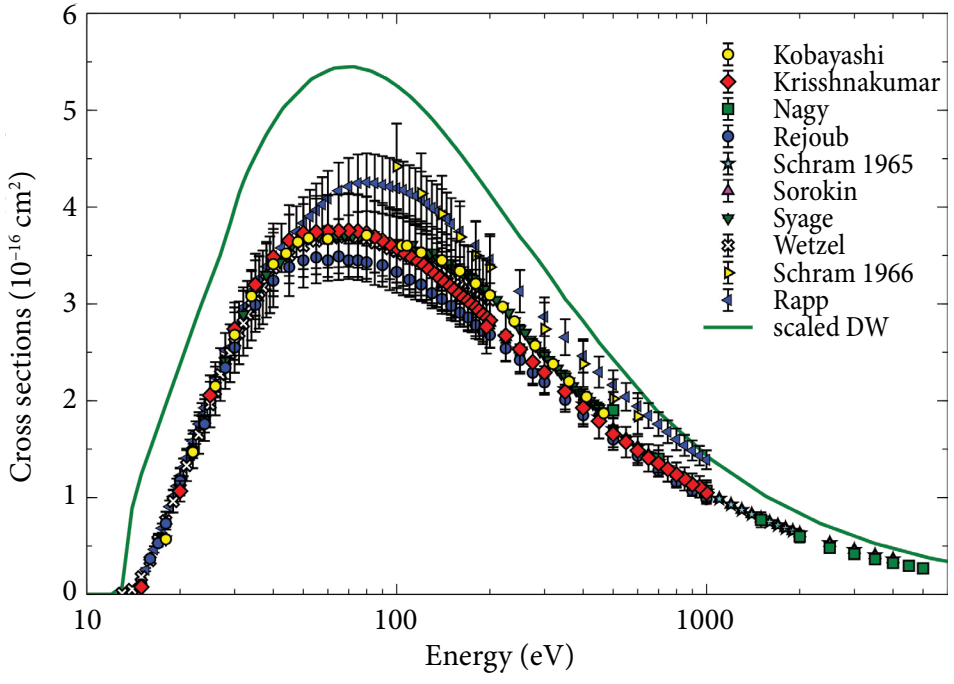

Fig. 3. Scaled DW cross sections compared to the experimental data. DW cross sections obtained in the potential of the ionizing ion.

Ionization cross sections calculated using the ionization threshold recommended by NIST are compared to the measurements [10–19] in Fig. 4. It is clearly seen that there is a fairly good agreement of theoretical data with the measurements from the ionization threshold up to ~50 eV where the ionization to the Kr^{2+} states starts to appear on the scene [19].

As mentioned before, there are two groups of published experimental data. One group presents total ionization cross sections not separating the production of higher ionization stages [10–12]. Other group is the partial ionization cross sections for produced ions [13–19]. We present the ionization cross sections calculated for the transitions

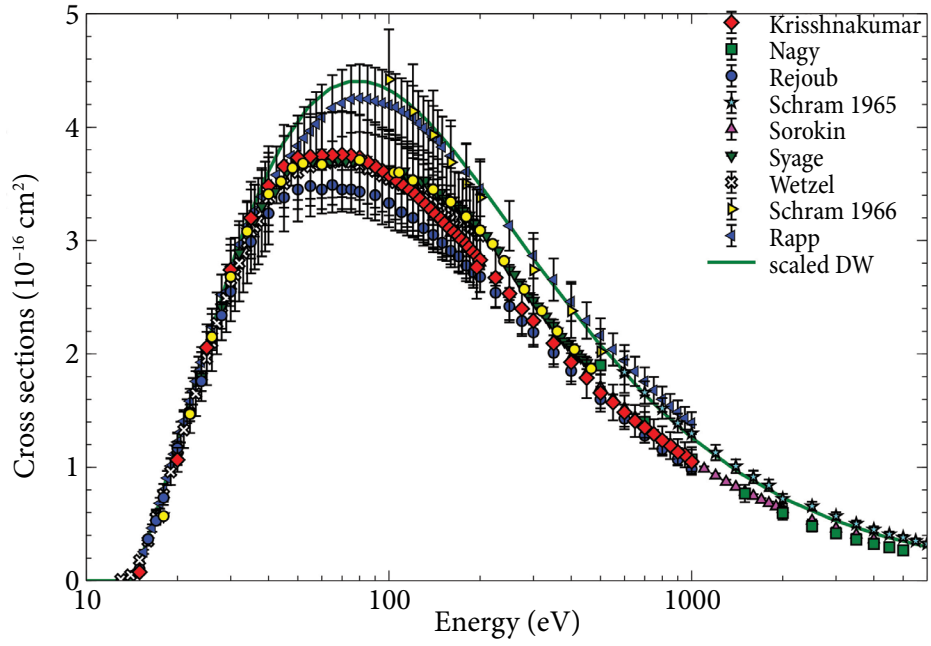

Fig. 4. Scaled DW cross sections compared to the experimental data. DW cross sections obtained in the potential of the ionizing ion. The single ionization threshold is taken equal to the NIST value.

from the ground level of the Kr atom to the states of the Kr^+ ion. However, there is the possibility that scattered or ejected electrons can remove additional electrons from the atomic system on their way out. This means that the calculated single ionization cross sections have to be corrected by the cross sections transferred to the higher ionization stages [36, 42]. The theoretical cross sections are compared to the experimental data and this corresponds to the total ionization process in Fig. 5. An incredibly

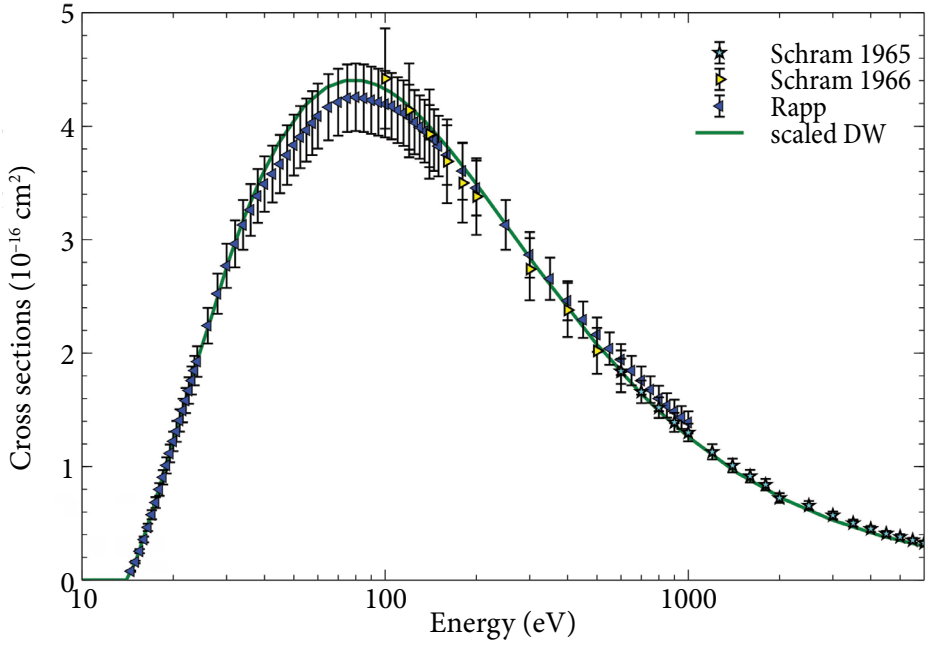

Fig. 5. Scaled DW cross sections compared to the experimental data. DW cross sections obtained in the potential of the ionizing ion. The single ionization threshold is taken equal to the NIST value. The experimental data corresponds to the total ionization cross sections.

good agreement with the measurements is obtained for the theoretical cross sections.

It should be noted that the indirect process contributes ~2% to the peak of the ionization cross sections when the NIST ionization threshold is used in calculations (Fig. 5). No contribution of excitations from the 4*p* subshells is obtained in this case. The study that uses the theoretical ionization threshold leads to ~15% for EA. The EA 4*p* channel produces ~11% for the peak value.

4. Conclusions

Electron-impact ionization cross sections are studied for the ground level of the Kr atom using the scaled DW approximation. The ionization threshold provided by NIST is used to obtain the final cross sections. Fairly good agreement is obtained with the total ionization measurements that include the single and higher ionization stages produced by electron impact. This demonstrates that the higher ionization stages appear as a result of the kick-off of additional electrons from the atomic system by scattered or ejected electrons after the first impact. The study shows that the contribution from the indirect process is negligible for the single ionization cross sections (~2%). The main contribution to the total ionization process is obtained from the CI 4*p* channel.

Acknowledgements

Part of the computations were performed on the High Performance Computing (HPC) Cluster at the Institute of Theoretical Physics and Astronomy, Faculty of Physics, Vilnius University. This project has received partial funding from the Research Council of Lithuania (LMTLT), Agreement No. S-SV-24-226.

References

[1] W.P. Bidelman, Line identifications in peculiar stars, Astron. J. **67**, 111 (1962), https://doi.org/10.1086/108637

[2] J.A. Cardelli and D.M. Meyer, The abundance of interstellar krypton*, Astrophys. J. **477**, L57 (1997), https://doi.org/10.1086/310513

[3] S.I.B. Cartledge, J.T. Lauroesch, D.M. Meyer, U.J. Sofia, and G.C. Clayton, Interstellar krypton abundances: The detection of kiloparsec-scale differences in galactic nucleosynthetic history*, Astrophys. J. **687**, 1043 (2008), https://doi.org/10.1086/592132

[4] D. Pequignot and J.P. Baluteau, The identification of krypton, xenon and other elements of rows 4, 5 and 6 of the periodic table in the planetary nebula NGC 7027*, Astron. Astrophys. **283**(2), 593–625 (1994).

[5] K. Werner, T. Rauch, E. Ringat, and J.W. Kruk, First detection of krypton and xenon in a white dwarf, Astrophys. J. Lett. **753**(1), L7 (2012), https://doi.org/10.1088/2041-8205/753/1/L7

[6] J. Flicstein, Y. Vitel, O. Dulac, C. Debauche, Y. Nissim, and C. Licoppe, Tunable UV-flash krypton lamp array useful for large area deposition and in situ UV annealing of Si-based dielectrics, Appl. Surf. Sci. **86**(1–4), 286–293 (1995), https://doi.org/10.1016/0169-4332(94)00458-7

[7] F.N. Haddou, P. Guillot, A. Belasri, T. Maho, and B. Caillier, Formation of low pressure striations in a krypton lamp, experimental characterization of the discharge: Spectroscopic and electrical analysis, Optik **241**, 166339 (2021), https://doi.org/10.1016/j.ijleo.2021.166339

[8] Q. Liu, R. Wang, Z. Yang, J. Sun, W. Yang, H. Wang, and X. Xu, Demonstration of a diode-pumped dual-wavelength metastable krypton laser, High Power Laser Sci. Eng. **11**, e87 (2023), https://doi.org/10.1017/hpl.2023.73

[9] Y.E. Chung, S.R. Hong, M.-J. Lee, M. Lee, and H.-J. Lee, Krypton-enhanced ventilation CT with dual energy technique: Experimental study for optimal krypton concentration, Exp. Lung Res. **40**(9), 439–446 (2014), https://doi.org/10.3109/01902148.2014.946630

[10] D. Rapp and P. Englander-Golden, Total cross sections for ionization and attachment in gases by electron impact. I. Positive ionization, J. Chem. Phys. **43**, 1464–1479 (1965), https://doi.org/10.1063/1.1696957

[11] B. Schram, F. De Heer, M. van der Wiel, and J. Kistemaker, Ionization cross sections for

electrons (0.6–20 keV) in noble and diatomic gases, Phys. **31**(1), 94–112 (1965).

[12] B. Schram, H. Moustafa, J. Schutten, and F. de Heer, Ionization cross sections for electrons (100–600 eV) in noble and diatomic gases, Phys. **32**(4), 734–740 (1966), https://doi.org/10.1016/0031-8914(66)90005-X

[13] P. Nagy, A. Skutlartz, and V. Schmidt, Absolute ionisation cross sections for electron impact in rare gases, J. Phys. B **13**, 1249 (1980), https://doi.org/10.1088/0022-3700/13/6/028

[14] R.C. Wetzel, F.A. Baiocchi, T.R. Hayes, and R.S. Freund, Absolute cross sections for electron-impact ionization of the rare-gas atoms by the fast-neutral-beam method, Phys. Rev. A **35**, 559–577 (1987), https://doi.org/10.1103/PhysRevA.35.559

[15] E. Krishnakumar and S.K. Srivastava, Ionisation cross sections of rare-gas atoms by electron impact, J. Phys. B **21**, 1055 (1988), https://doi.org/10.1088/0953-4075/21/6/014

[16] J.A. Syage, Electron-impact cross sections for multiple ionization of Kr and Xe, Phys. Rev. A **46**, 5666–5679 (1992), https://doi.org/10.1103/PhysRevA.46.5666

[17] A.A. Sorokin, L.A. Shmaenok, S.V. Bobashev, B. Möbus, M. Richter, and G. Ulm, Measurements of electron-impact ionization cross sections of argon, krypton, and xenon by comparison with photoionization, Phys. Rev. A **61**, 022723 (2000), https://doi.org/10.1103/PhysRevA.61.022723

[18] A. Kobayashi, G. Fujiki, A. Okaji, and T. Masuoka, Ionization cross section ratios of rare-gas atoms (Ne, Ar, Kr and Xe) by electron impact from threshold to 1 keV, J. Phys. B **35**, 2087 (2002), https://doi.org/10.1088/0953-4075/35/9/307

[19] R. Rejoub, B.G. Lindsay, and R.F. Stebbings, Determination of the absolute partial and total cross sections for electron-impact ionization of the rare gases, Phys. Rev. A **65**, 042713 (2002), https://doi.org/10.1103/PhysRevA.65.042713

[20] E. McGuire, Electron ionization cross sections in the Born approximation, Phys. Rev. A **16**(1), 62–72 (1977), https://doi.org/10.1103/PhysRevA.16.62

[21] D. Margreiter, H. Deutsch, and T. Märk, A semi-classical approach to the calculation of electron impact ionization cross-sections of atoms: from hydrogen to uranium, Int. J. Mass Spectrom. **139**, 127–139 (1994), https://doi.org/10.1016/0168-1176(94)90024-8

[22] D.W. Chang and P.L. Altick, Doubly, singly differential and total ionization cross sections of rare-gas atoms, J. Phys. B **29**, 2325 (1996), https://doi.org/10.1088/0953-4075/29/11/020

[23] S.D. Loch, M.S. Pindzola, C.P. Ballance, D.C. Griffin, D.M. Mitnik, N.R. Badnell, M.G. O'Mullane, H.P. Summers, and A.D. Whiteford, Electron-impact ionization of all ionization stages of krypton, Phys. Rev. A **66**, 052708 (2002), https://doi.org/10.1103/PhysRevA.66.052708

[24] V. Jonauskas, Electron-impact double ionization of the carbon atom, A&A **620**, A188 (2018), https://doi.org/10.1051/0004-6361/201834303

[25] V. Jonauskas, Electron-impact single ionization of the nitrogen atom, A&A **659**, A11 (2022), https://doi.org/10.1051/0004-6361/202141801

[26] A. Kynienė, S. Kučas, S. Pakalka, Š. Masys, and V. Jonauskas, Electron-impact single ionization of Fe^{3+} from the ground and metastable states, Phys. Rev. A **100**, 052705 (2019), https://doi.org/10.1103/PhysRevA.100.052705

[27] V. Jonauskas, Electron impact single ionization for Si atom, At. Data Nucl. Data Tables **135–136**, 101363 (2020), https://doi.org/10.1016/j.adt.2020.101363

[28] R.D. Cowan, *The Theory of Atomic Structure and Spectra* (University of California Press, Berkeley, CA, 1981), https://doi.org/10.1525/9780520906150

[29] Y.-K. Kim, Scaling of plane-wave Born cross sections for electron-impact excitation of neutral atoms, Phys. Rev. A **64**, 032713 (2001), https://doi.org/10.1103/PhysRevA.64.032713

[30] Y.-K. Kim and J.-P. Desclaux, Ionization of carbon, nitrogen, and oxygen by electron impact, Phys. Rev. A **66**, 012708 (2002), https://doi.org/10.1103/PhysRevA.66.012708

[31] D.-H. Kwon, Y.-J. Rhee, and Y.-K. Kim, Cross sections for ionization of Mo and Mo^+ by

electron impact, Int. J. Mass Spectrom. **245**(1–3), 26–35 (2005), https://doi.org/10.1016/j.ijms.2005.06.007

[32] D.-H. Kwon, Y.-J. Rhee, and Y.-K. Kim, Ionization of W and W^+ by electron impact, Int. J. Mass Spectrom. **252**(3), 213–221 (2006), https://doi.org/10.1016/j.ijms.2006.03.007

[33] M.F. Gu, The flexible atomic code, Can. J. Phys. **86**, 675–689 (2008), https://doi.org/10.1139/p07-197

[34] A. Kramida, Yu. Ralchenko, J. Reader, and NIST ASD Team, *NIST Atomic Spectra Database*, Version 5.11 (National Institute of Standards and Technology, Gaithersburg, MD, 2024), https://physics.nist.gov/asd

[35] J. Koncevičiūtė, S. Kučas, Š. Masys, A. Kynienė, and V. Jonauskas, Electron-impact triple ionization of Se^{2+}, Phys. Rev. A **97**, 012705 (2018), https://doi.org/10.1103/PhysRevA.97.012705

[36] S. Pakalka, S. Kučas, Š. Masys, A. Kynienė, A. Momkauskaitė, and V. Jonauskas, Electron-impact single ionization of the Se^{3+} ion, Phys. Rev. A **97**, 012708 (2018), https://doi.org/10.1103/PhysRevA.97.012708

[37] J. Koncevičiūtė, S. Kučas, A. Kynienė, Š. Masys, and V. Jonauskas, Electron-impact double and triple ionization of Se^{3+}, J. Phys. B **52**(2), 025203 (2019), https://doi.org/10.1088/1361-6455/aaf3e6

[38] A. Kynienė, S. Pakalka, Š. Masys, and V. Jonauskas, Electron-impact ionization of W^{25+}, J. Phys. B **49**(18), 185001 (2016), https://doi.org/10.1088/0953-4075/49/18/185001

[39] A. Kynienė, Š. Masys, and V. Jonauskas, Influence of excitations to high-*nl* shells for the ionization process in the W^{26+} ion, Phys. Rev. A **91**, 062707 (2015), https://doi.org/10.1103/PhysRevA.91.062707

[40] A. Kynienė, G. Merkelis, A. Šukys, Š. Masys, S. Pakalka, R. Kisielius, and V. Jonauskas, Maxwellian rate coefficients for electron-impact ionization of W^{26+}, J. Phys. B **51**(15), 155202 (2018), https://doi.org/10.1088/1361-6455/aacd87

[41] V. Jonauskas, A. Kynienė, G. Merkelis, G. Gaigalas, R. Kisielius, S. Kučas, Š. Masys, L. Radžiūtė, and P. Rynkun, Contribution of high-*nl* shells to electron-impact ionization processes, Phys. Rev. A **91**, 012715 (2015), https://doi.org/10.1103/PhysRevA.91.012715

[42] V. Jonauskas, Electron-impact ionization of Se^{4+}, J. Quant. Spectrosc. Radiat. Transf. **239**, 106659 (2019), https://doi.org/10.1016/j.jqsrt.2019.106659

Kr ATOMO JONIZACIJA ELEKTRONŲ SMŪGIAIS

A. Kynienė, V. Paberžis, Š. Masys, V. Jonauskas

Vilniaus universiteto Teorinės fizikos ir astronomijos institutas, Vilnius, Lietuva

Santrauka

Darbe nagrinėjami elektronų smūgiais pasiektos jonizacijos skerspjūviai Kr atomo pagrindiniam lygmeniui, naudojant iškraipytųjų bangų (IB) metodą su daugiklio funkcijomis. IB jonizacijos skerspjūviai, apskaičiuoti jonizuojančio jono potenciale, pervertina eksperimentinius duomenis esant žemoms ir vidutinėms elektronų energijoms. IB rezultatai su daugiklio funkcijomis, kai įtraukiama Nacionalinio standartų ir technologijos instituto pateikta jonizacijos slenksčio vertė, gerai sutampa su atliktais matavimais. Galutiniai rezultatai rodo nereikšmingą netiesioginių jonizacijos procesų indėlį į bendrą jonizacijos, pasiektos elektronų smūgiais, skerspjūvį. Atliktas tyrimas atskleidžia, kad aukštesnės jonizacijos būsenos atsiranda dėl papildomų elektronų išmetimo iš atominės sistemos, vykstant papildomai jonizacijai.